Journal of Global Optimization, 11, 35–53 (1997)

Global Optima of Lennard-Jones Clusters

ROBERT H. LEARY*
San Diego Supercomputer Center, San Diego, CA 92138, URL: http://www.sdsc.edu/~leary, Email: leary@sdsc.edu.

Abstract. This paper summarizes the current state of knowledge concerning putative global minima of the potential energy function for Lennard-Jones clusters, an intensely studied molecular conformation problem. Almost all known exceptions to global optimality of the well-known *Northby multilayer icosahedral conformations* for microclusters are shown to be minor variants of that geometry. The truly exceptional case of face-centered cubic lattice conformations is examined and connections are made with the macrocluster problem. Several types of algorithms and their limitations are explored, and a new variation on the growth sequence idea is presented and shown to be effective for both small and large clusters.

Keywords: Molecular conformation, global optimization, Lennard-Jones cluster.

1. Introdnction

Perhaps the most intensely studied molecular conformation problem is that of Lennard-Jones microclusters. The term microcluster is used to designate an aggregate of particles sufficiently small that a significant fraction of the particles are present on the surface and hence the cluster energy is not dominated by bulk interior effects. Here we will be primarily concerned with *microclusters of N neutral atoms* in the range $2 \leq N \leq 147$, interacting pairwise via the Lennard-Jones potential function, as well as large macroclusters significantly beyond this range. The goal is to characterize the current state of knowledge regarding putative global optima of the full Lennard-Jones potential function consisting of the sum of $N(N-1)/2$ pairwise interaction terms.

The global optimization of Lennard-Jones clusters (GOLJC) problem has attracted interest for a variety of reasons:

a) GOLJC is a very simple yet reasonably accurate mathematical model of a real physical system, namely that of low temperature microclusters of heavy rare gas atoms such as argon, krypton, or xenon. Thus results from simulations can be compared directly with laboratory measurements. *In general, there is good agreement* between the overall character of current global optimization results and that of physical measurements from electron diffractometry [16] and mass spectrometry [18], both in terms of microcluster geometry as well as magic numbers corresponding to particularly favorable cluster sizes. Also, as N grows beyond the microclus-

*THE RESEARCH OF THIS AUTHOR WAS SUPPORTED IN PART BY NATIONAL SCIENCE FOUNDATION GRANT ASC-8902825

ter range, computer models based on this same potential have been successful in predicting the transition from non-crystalline microcluster geometry to bulk face-centered cubic (FCC) crystalline forms. The solutions also have connections with current research in several areas of physics, chemistry, and materials science, including metallic and molecular clusters, quasicrystals and other non-crystalline solids, and liquids [18].

b) The problem is simple to state and easily simulated by computer, yet challenging and complex in the behavior of its solutions. The objective function is non-convex and the number of energetically distinct local optima is believed to grow at least exponentially with N [9, 15]. However, good putative global optima are known over the entire microcluster range and new results are still being found within this range. Thus the problem is both a benchmark for global optimization methods as well as an open research area.

c) Some features are common to both GOLJC and protein folding models, an area of great current interest. For example, both include Lennard-Jones interactions as a significant contribution to the potential, and there is some evidence that there are qualitative similarities in the overall energy landscapes which might make algorithms transferable from one to the other.

GOLJC is concerned with finding a minimum potential energy conformation of a static cluster of N identical atoms interacting pairwise via the Lennard-Jones potential. A conformation is a point in the $3N$-dimensional space of coordinates of atomic centers. For a single pair of atoms, the Lennard-Jones potential in reduced units is given by

$$u(r) = r^{-12} - 2r^{-6} \tag{1}$$

where r is the Euclidean interatomic distance. This potential, graphed in Figure 1, is the difference between an *ad hoc* repulsive term r^{-12}, representing a strong but short range core repulsive force that prevents the atomic centers from approaching each other at distances significantly less than an atomic diameter, and a longer range attractive term $2r^{-6}$, due to the van der Waals force between neutral atoms. This latter term, also known as the induced dipole-dipole interaction, is a quantum effect and the $O(r^{-6})$ dependency is theoretically correct to first order [13]. Note that the pair potential has been scaled so that the minimum occurs at $r = 1$ with corresponding potential energy $u(1) = -1$. For $N > 2$, pairwise additivity is assumed, so the GOLJC problem becomes that of minimizing, over the $3N$-dimensional space of atomic coordinates, the total potential energy

$$U = \sum_{i=1}^{N-1} \sum_{j=i+1}^{N} u(r_{ij}) \tag{2}$$

where r_{ij} is the distance between atoms i and j in reduced units.

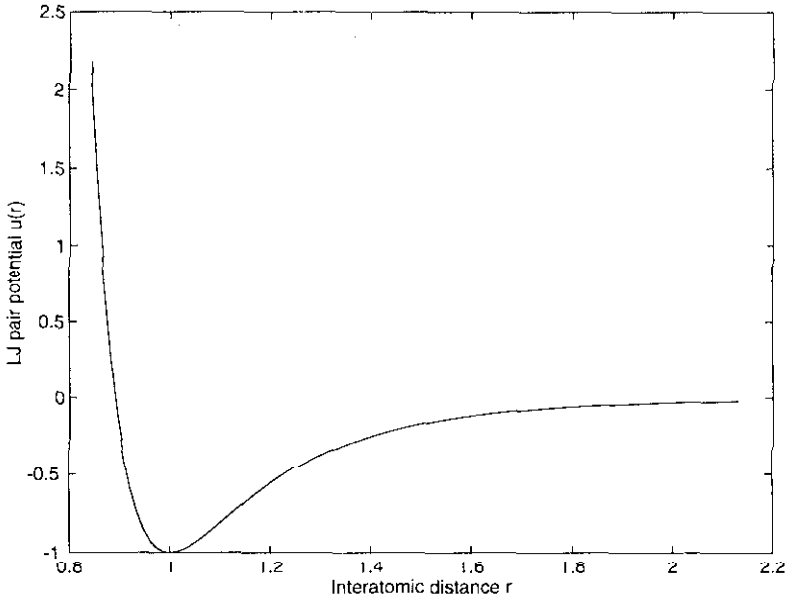

Figure 1. The Lennard-Jones pair potential function.

In section 2 we discuss the growth sequence ideas that eventually led to the well-known results of Northby [19], which established multilayer icosahedral (MIC) conformations as the dominant structural motif for optimal microclusters and produced putative global optima for all $N \leq 147$. Many authors have found instances of conformations with lower energies than those of Northby, and there are now known to be at least fifteen values of N for which the original Northby conformations are not global optima. We present all of the best currently known putative microcluster global optima, and show that these fall into several general geometric classes, all but one of which are closely related to the original Northby MIC geometry. In a new result, the idea of a minimal growth sequence is reversed to find many of the microcluster global optima where the Northby results are known to be non-optimal, including one class on which more general "build-up" algorithms based on forward growth sequences generally fail. The final class of polyhedral FCC lattice structures is then discussed, and connections are made with optimal forms for large clusters. Section 3 considers general purpose algorithms for the microcluster problem that make no prior assumptions regarding optimal cluster geometry, yet are successful in finding most microcluster global optima. Section 4 contains some concluding remarks on the successes and limitations of current algorithms.

2. Growth Sequence and Lattice Methods

2.1. Putative Global Minima

Tables 1 and 2 presents a list of the best current putative global minima for $2 \leq N \leq 147$. Hereafter we shall refer to these simply as global minima or optima with the understanding that no better values are known, and denote the optimal cluster of size N as **N**. The underlying conformations corresponding to the listed binding energy values U are organized into several geometric classes, including the

Table 1. Putative global optima of Lennard-Jones clusters $2 \leq N \leq 75$. (*) denotes an improved energy value relative to the original Northby conformations.

N	$-U$	Conform.	R	N	$-U$	Conform.	R
2	1.000000			39	180.033185	MIC(IC)	
3	3.000000	-	2	40	185.249839	MIC(IC)	39
4	6.000000	PT	3	41	190.536277	MIC(IC)	40
5	9.103852	PT	4	42	196.277534	MIC(IC)	41
6	12.712062	FCC		43	202.364664	MIC(IC)	42
7	16.505384	PT		44	207.688728	MIC(IC)	43
8	19.821489	PT	7	45	213.784862	MIC(IC)	44
9	24.113360	PT	8	46	220.680330	MIC(IC)	45
10	28.422532	PT	9	47	226.012256	MIC(IC)	46
11	32.765970	PT	10	48	232.199529	MIC(IC)	47
12	37.967600	PT	11	49	239.091864	MIC(IC)	48
13	44.326801	MIC(IC)	12	50	244.549926	MIC(IC)	49
14	47.845157	MIC(FC)	13	51	251.253964	MIC(IC)	
15	52.322627	MIC(FC)	14	52	258.229991	MIC(IC)	51
16	56.815742	MIC(FC)	15	53	265.203016	MIC(IC)	52
17	61.317995	MIC(FC)	16	54	272.208631	MIC(IC)	53
18	66.530949	MIC(FC)		55	279.248470	MIC(IC)	54
19	72.659782	MIC(FC)	18	56	283.643105	MIC(IC)	55
20	77.177043	MIC(FC)	19	57	288.342625	MIC(FC)	
21	81.684571	MIC(FC)	20	58	294.378148	MIC(FC)	57
22	86.809782	MIC(FC)	21	59	299.738070	MIC(FC)	
23	92.844472	MIC(FC)	22	60	305.875476	MIC(FC)	59
24	97.348815	MIC(FC)	23	61	312.008896	MIC(FC)	
25	102.372663	MIC(FC)	24	62	317.353901	MIC(FC)	
26	108.315616	MIC(FC)	25	63	323.489733	MIC(FC)	62
27	112.873584	MIC(FC)		64	329.620147	MIC(FC)	63
28	117.822401	MIC(FC)	27	65	*334.971532	MIC(FC)	
29	123.587371	MIC(FC)	28	66	*341.110599	MIC(FC)	
30	128.286570	MIC(FC)		67	347.252006	MIC(FC)	66
31	133.586422	MIC(IC)		68	353.394542	MIC(FC)	
32	139.635523	MIC(IC)	31	69	*359.882566	MISV(FC)	68
33	144.842719	MIC(IC)	32	70	366.892251	MIC(FC)	69
34	150.044528	MIC(IC)	33	71	373.349660	MIC(FC)	70
35	155.756643	MIC(IC)		72	*378.637253	HOC(FC)	71
36	161.825362	MIC(IC)	35	73	384.789377	MIC(FC)	
37	167.033672	MIC(IC)	36	74	390.908500	MIC(FC)	73
38	*173.928427	FCC		75	*396.282249	HOC(FC)	74

Table 2. Putative global optima of Lennard-Jones clusters $76 \leq N \leq 147$. (*) denotes an improved energy value relative to the original Northby conformations.

N	$-U$	Conform.	R	N	$-U$	Conform.	R
76	*402.384580	MIC(FC)		112	634.874596	MIC(IC)	111
77	*408.518265	MIC(FC)	76	113	*641.794704	MISV(IC)	
78	*414.794401	MISV(FC)		114	648.833100	MIC(IC)	113
79	421.810897	MIC(FC)	78	115	*655.756307	MISV(IC)	
80	428.083564	MIC(FC)	79	116	662.809353	MIC(IC)	115
81	434.343643	MIC(FC)	80	117	668.282701	MIC(IC)	116
82	440.550425	MIC(IC)		118	674.769635	MIC(IC)	117
83	446.924094	MIC(IC)	82	119	681.419158	MIC(IC)	118
84	452.657214	MIC(IC)		120	687.021966	MIC(IC)	119
85	459.055799	MIC(FC)		121	693.819577	MIC(IC)	
86	465.384493	MIC(IC)		122	700.939379	MIC(IC)	121
87	472.098164	MIC(IC)		123	707.802109	MIC(IC)	
88	*479.032629	MISV(IC)		124	714.920896	MIC(IC)	123
89	486.053911	MIC(IC)	88	125	721.303235	MIC(IC)	124
90	492.433908	MIC(IC)	89	126	727.349853	MIC(IC)	
91	498.811060	MIC(IC)	90	127	734.479629	MIC(IC)	126
92	505.185309	MIC(IC)	91	128	741.332100	MIC(IC)	
93	510.877687	MIC(IC)		129	748.460615	MIC(IC)	128
94	517.264131	MIC(IC)	93	130	755.271073	MIC(IC)	
95	523.640211	MIC(IC)	94	131	762.441556	MIC(IC)	130
96	529.879146	MIC(IC)		132	768.042102	MIC(IC)	131
97	536.681383	MIC(IC)	96	133	775.023203	MIC(IC)	
98	*543.642957	MISV(IC)		134	*782.206157	MIC(IC)	133
99	550.666526	MIC(IC)	98	135	790.278120	MIC(IC)	
100	557.039819	MIC(IC)	99	136	797.453259	MIC(IC)	135
101	563.411234	MIC(IC)	100	137	804.631473	MIC(IC)	136
102	569.277723	MIC(IC)		138	811.812780	MIC(IC)	137
103	575.658879	MIC(IC)	102	139	818.993848	MIC(IC)	138
104	582.038429	MIC(IC)	103	140	826.174676	MIC(IC)	139
105	588.266501	MIC(IC)		141	833.358586	MIC(IC)	140
106	595.061072	MIC(IC)	105	142	840.538610	MIC(IC)	141
107	*602.007110	MISV(IC)		143	847.721698	MIC(IC)	142
108	609.033010	MIC(IC)	107	144	854.904499	MIC(IC)	143
109	615.411166	MIC(IC)	108	145	862.087012	MIC(IC)	144
110	621.788174	MIC(IC)	109	146	869.272572	MIC(IC)	145
111	628.068416	MIC(IC)		147	876.461207	MIC(IC)	146

polytetrahedral (PT) structures of Hoare and Pal [10], the IC and FC multilayer icosahedral lattice conformations (MIC(FC) and MIC(IC)) of Northby, two classes of minor variants of the Northby structures (MISV for Missing Inner Shell Vertex and HOC for half octahedral cap), and FCC (face-centered cubic) lattice strnctures. Also, for each **N**, it is noted when **N-1** can be obtained by application of a simple reverse greedy operator **R**, as explained below.

2.2. Growth Sequences

The most successful early GOLJC computer simulations were dominated by the idea of growth sequences - that is, candidate global optima of size N may be built up by adding an atom at packing vertices above the surface of previously generated structures of size $N-1$. Once a new structure is generated, it is relaxed to a nearby stable conformation by a local optimization algorithm. (We note that in the molecular conformation literature, a distinction is made between stable states, corresponding to local minima characterized by a positive definite Hessian matrix of U, and metastable states, which are stationary saddle points. Depending on the local optimizer used for the relaxation step, a check may be necessary to confirm the stability of the conformation). If at a given stage, several unrelaxed conformations with different energies can be generated by different placements of the added atom, the placement resulting in the lowest energy unrelaxed conformation is selected - i.e. a "greedy" step is used. The selected conformation is then relaxed. Thus starting from any given seed structure of size N, successive application of this forward greedy operator defines a chain of stable conformations of increasing size called a minimal growth sequence.

Hoare and Pal [10] were the first to apply this idea systematically in a computer simulation with the full LJ potential using all $N(N-1)/2$ interaction terms. Their starting seed was the regular unit tetrahedron with atoms at the vertices, the obvious global minimum conformation for $N = 4$. At each stage atomic additions were considered at the tetrahedral capping position over each triangular face of the current structure. Thus all structures in the growth sequence consist of multiple tetrahedra joined at shared faces. The first structure above the seed is the globally optimal trigonal bi-pyramid (or bi-tetrahedron) at $N = 5$, followed by the tri-tetrahedron at $N = 6$, one of two known local minima (the other is the octahedron, which is not a polytetrahedron and is in fact the global optimum). Up to this point, all faces of the starting polytetrahedra have been equivalent so there has been only one candidate for the next conformation in the chain. However, the tri-tetrahedron has several non-equivalent faces, leading to three different stable polytetrahedral conformations at $N = 7$. The best of these is the pentagonal bi-pyramid, a structure with a five-fold axis of symmetry, which is the global optimum.

Hoare and Pal followed the polytetrahedral minimal growth sequence out to $N = 66$. They compared this sequence with that produced from the globally optimal $N = 6$ octahedral seed (using tetrahedral capping over triangular faces and half-octahedral capping over square faces) and found that the polytetrahedral sequence energies are always lower for $N > 6$. With the exception of $N = 6$ and $N = 17$, it produces global optima for $4 \leq N \leq 21$. Hoare and Pal also followed the alternate polytetrahedral growth sequence seeded by the second best polytetrahedral local minimum at $N = 7$. The energies of this sequence cross under those of original sequence at $N = 23$ and stay below it until $N = 32$, with several additional

crossings up to $N = 66$. This second sequence is now known to produce global optima at $N = 25$ and $N = 26$. However, neither sequence produces any further global optima and for values above $N = 35$, both are quite far from the best known results.

Many of the optimal microclusters in Tables 1 and 2 are connected by forward growth sequences in the sense that $\mathbf{F(N) = N+1}$, where **F** is a general greedy forward growth operator that searches over a more extensive set of coordinates than just tetrahedral capping positions. $\mathbf{F(N)}$ may be defined as the conformation resulting from a 3-dimensional energy minimization over coordinates of a single added atom, followed by a relaxation over the full $3N$ coordinates to a local minimum. Thus **F** itself involves a low-dimensional global optimization, although in practice the search is often limited to sampling near the cluster surface.

It is also possible to define a reverse greedy operator **R** which removes the *least tightly bound atom* in a conformation of N atoms, followed by relaxation to a local minimum conformation of $N - 1$ atoms. The energy contribution u_i of atom i to a cluster of size N is one half of the energy of all the $N - 1$ pairwise interactions involving that atom, i.e.

$$u_i = \frac{1}{2} \sum_{j \neq i} u(r_{ij}). \tag{3}$$

It is easily verified that the total potential energy is given by

$$U = \sum_{i=1}^{N} u_i. \tag{4}$$

The least tightly bound atom in a microcluster is defined as the atom with the maximum value of u_i. (Binding energy is the negative of potential energy; hence the least tightly bound atom has the lowest binding energy contribution). The operator **R** also often produces global optima from global optima, as can be seen from Table 1. Note that the forward and reverse greedy operators are usually but not always inverses of each other.

While variants of the forward operator have been exploited in many algorithms, the use of the reverse operator is apparently new. For example, the optimal structure **78** in Table 2 obtained by **R** has not been previously reported. Moreover, in eight of the fifteen instances where the original Northby conformations have been found to be non-optimal, the global optima conformations can be found by applications of **R** to other MIC global optima. We believe **R** is also a powerful tool for locating optima or approximate optima for very large lattice structures. As described below, a large non-optimal starting lattice conformation may be repeatedly pruned by **R** to eventually yield an optimal or near optimal conformation.

2.3. Multilayer Icosahedral Lattice Models

Mackay [17] first constructed a class of icosahedral packings by adding successively larger icosahedral shells in layers around a core central atom (Figure 2). Atoms within each triangular face are placed in staggered rows in a two dimensional hexag-

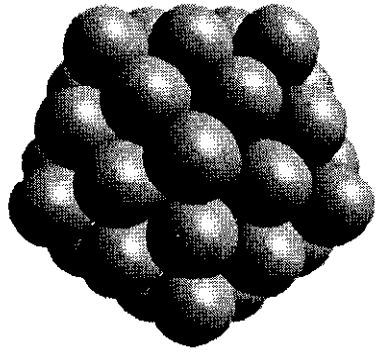

Figure 2. Mackay icosahedral conformation for $N = 55$.

onal close-packed arrangement. Each atom in the interior of a face in a given shell is in a tetrahedral capping position relative to three atoms in the underlying shell. The magic numbers $N = 13$, 55, and 147 correspond to the total number of atoms in one, two and three-shell Mackay icosahedra, respectively. Based in part on earlier work by Farges *et al.* [7], Northby [19] suggested that global optima for the GOLJC problem could be obtained by relaxing structures built on the Mackay icosahedral lattice, called the IC lattice by Northby, or a slight modification called the FC lattice. This second lattice differs from the IC latttice only in the outer shell, which maintains icosahedral symmetry and consists of points at the icosahedral vertices and the *stacking fault positions* of the outer IC shell. These are alternate tetrahedral capping positions over the next to outermost shell; the union of the outer FC and IC shells contains all possible such positions. We shall refer to these two variants of the overall MIC lattice as MIC(IC) and MIC(FC) to emphasize the layered icosahedral nature of each.

Northby formalized this idea with an algorithm that generates candidate structures for relaxation by a lattice optimization procedure. For non-magic numbers N, atoms are first used to fill as many inner MIC shells as possible. Remaining atoms are then placed in the outer IC or FC shell with a lattice search procedure in which both the full LJ potential as well as a simplified nearest neighbor potential are minimized. The global optima for each potential and each outer shell type are then relaxed and the best resulting structure chosen as the putative global optimum for the GOLJC problem.

The algorithm proved remarkably effective. For all $12 \leq N \leq 147$, it equaled or bettered all previously known putative global optima and produced over 120 completely new conformations. Even after extensive subsequent computational investigation, there are only fifteen values ($N = 38$, 65, 66, 69, 72, 75, 76, 77, 78, 88, 98, 107, 113, 115, and 134) in this range for which better values have been found. A modified version fo the Northby algorithm was introduced by Xue [27], who noted that in a small fraction of cases a higher-lying local optimizer of the outer shell lattice optimization procedure relaxed to a better value than the global minima of that procedure. By adding local lattice minimizers to the starting candidate pool, Xue found improved optima for $N = 65$, 66, 75, 76, 77, and 134, although the improved value for $N = 75$ is now known not to be a global optimum. However, the Xue algorithm finds all known instances in the range $13 \leq N \leq 147$ where the global optimum conforms to the original Northby MIC lattice model. Xue also improved the performance of the algorithm, so it is fast and scales well to structures as large as $N = 100{,}000$ [26]. However, the results for very large clusters are now known to be only local local minima in the class of MIC structures and well above the best FCC structures of the same size in energy [11, 14, 21, 23, 25].

The remaining ten cases for $N > 13$ where Northby MIC conformations are not global optima for microclusters fall into three geometric classes. All seven members **69**, **78**, **88**, **98**, **107**, **113** and **115** of the missing inner shell vertex (MISV) class can be obtained by the reverse greedy operator **R**. Although the least tightly bound atom is usually on the surface, it does not necessarily belong to the outer shell. Typically atoms in the partially filled outer shell tend to aggregate in a compact cap which only partially covers the underlying filled shell. Uncovered vertex atoms in this underlying shell may be the least tightly bound atom in the relaxed cluster. Upon removal of this inner shell vertex atom, the resulting structure no longer conforms to the original Northby MIC model of complete inner shells. Figure 3 illustrates the relaxed optimal MISV conformation **78**. We note that an eighth MISV conformation at $N = 38$, obtained by removing an uncovered first shell vertex atom in **39**, is better than the best $N = 38$ MIC conformation. However, as shall be seen below, an FCC conformation is optimal for this case.

The second class of modified MIC structures which do not conform entirely to the Northby model are the global optima conformations **72** (Figure 4) and **75** with a half octahedral cap on the outer shell. Four of the six atoms in the stacking fault positions on adjacent outer FC faces in the MIC(FC) Northby structures **71** and **74**, respectively, lie approximately at the corners of a square. The pocket inside this square is an energetically attractive position for an additional atom, which forms a half-octahedral cap to the outer shell. This class of structures only becomes possible with three or more-shell configurations ($N > 55$) with an outer FC shell.

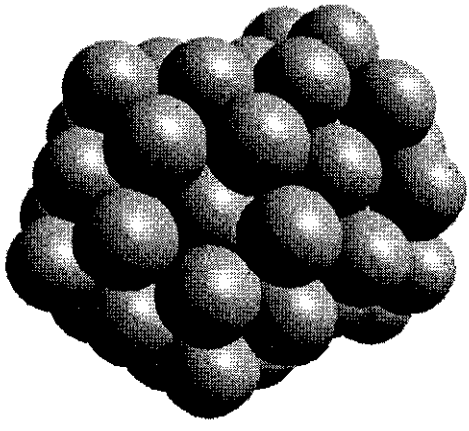

Figure 3. MISV conformation **78**. Note the missing vertex atom at the center, and the outer shell atoms at the upper right.

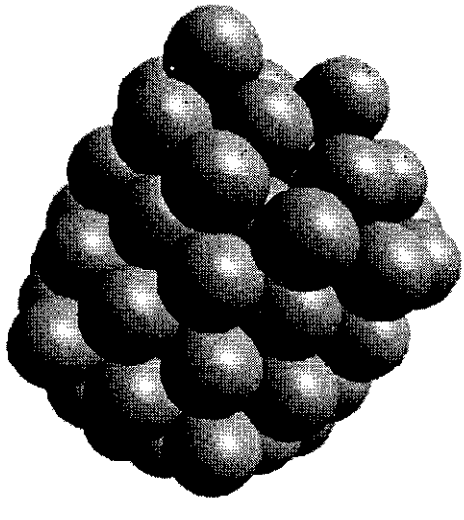

Figure 4. HOC conformation **72**. The half octahedral cap appears at top of cluster.

2.4. FCC Lattice Polyhedra

The last class of non-MIC optimal conformations includes **6** and **38** and is based on a true crystallographic face-centered cubic (FCC) rather than MIC lattice. An

even infinite FCC lattice with unit nearest neighbor spacing can be defined in 3-dimensional Euclidean space as

$$L_{even} = \{\frac{\sqrt{2}}{2}(i,j,k) : i+j+k \text{ is even, } i,j,k \text{ are integers}\} \tag{5}$$

The related odd FCC lattice L_{odd}, where the integer sum is odd, is simply a translate of the even lattice. Both can be considered as centered at the origin, which is a lattice point in the even lattice and a hole between lattice points in the odd lattice. Various polyhedral FCC lattice structures with K faces can be defined by intersection of even or odd FCC lattices with half spaces of the form

$$a_i x + b_i y + c_i z \leq d_i \tag{6}$$

for i=1, 2, ..., K. In particular the eight equivalent crystallographic (111) planes defined by $a = \pm 1$, $b = \pm 1$, $c = \pm 1$ for a fixed $d_i = d > 0$ bound an FCC octahedron. Similarly, the six (100) planes (a,b,c) = (1,0,0), (-1,0,0), (0,1,0), (0,-1,0), (0,0,1), and (0,0,-1) bound a cube, while the twelve (110) planes bound a rhombic dodecahedron. The notations (111), (100), and (110) are *Miller indices* [13] of classes of equivalent crystallographic planes. In the case of FCC lattices, these correspond to the coefficients of a particular member of the class.

Relaxed FCC polyhedra are believed to be optimal for large Lennard-Jones clusters. The infinite relaxed FCC latttice has the lowest known LJ energy per atom of any infinite crystallographic lattice structure [13] The classical Wulff construction [8] models the energy of large relaxed polyhedral clusters of size N on a crystallographic lattice as

$$U = NU_{inf} + \sum_{i=1}^{K} \gamma_i S_i \tag{7}$$

where U_{inf} is the average energy per atom in the relaxed infinite lattice, S_i is the surface area of face i, and $\gamma_i > 0$ is the *surface free energy* (also called the *excess surface energy* or simply *surface energy*) of plane i. Surface free energy is defined as the binding energy per unit area lost at the surface of a relaxed semi-infinite lattice bounded by a particular crystallographic plane relative to the binding energy in a relaxed infinite lattice [2]. Wulff showed that the optimal shape for lattice polyhedra is defined by the first order optimality condition (obtained from a Lagrange multiplier argument)

$$\frac{d_i}{\sqrt{{a_i}^2 + {b_i}^2 + {c_i}^2}} \propto \gamma_i \tag{8}$$

i.e., the distance from each facial plane i to the origin in the optimal polyhedral shape is proportional to the surface free energy of that plane. Usually only a few of the lower surface free energy planes will be active in the optimal shape, as the

others will lie outside the polyhedron defined by the low energy planes. The Wulff shape is the best compromise between sphericity (low surface to volume ratio) and low average surface free energy, and is determined by the ratios of the surface free energies of the bounding facial planes.

For most FCC materials, $\gamma_{111} < \gamma_{100} < \gamma_{110}$ are the three lowest surface free energies and only (111), (100), and possibly (110) planes are active in the optimal shape [12]. If only (111) and (100) planes are active, the Wulff polyhedron is a truncated octahedron in which each of the six (100) planes cuts off one vertex of an octahedron. Thus six square pyramids are removed, with the size of the pyramids governed by the cutting depth parameter f which is the fraction of the altitude from the octahedron center to the vertex that is cut off. The resulting figure has eight favorable (111) faces and six somewhat less favorable (100) faces. The *tetrakaidecahedron*, one of thirteen semi-regular Archimedean solids [5], corresponds to the cutting depth $f = \frac{1}{3}$ and is the Wulff shape if a simple near neighbor broken bond model is used in the surface free energy calculation [12]. The smallest FCC tetrakaidecabedron relaxes to the global optimum **38**, which is shown in Figure 5. To our knowledge, the only global optimization algorithms that have

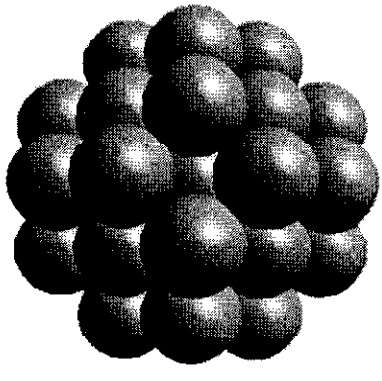

Figure 5. FCC tetrakaidecahedral conformation at $N = 38$.

found this structure are the general purpose algorithms in [6] and [15], which make no geometric assumptions, and the exponential tunneling algorithm in [1], which presupposes an FCC lattice. However, FCC tetrakaidecahedra have long been investigated and predicted to be optimal forms [12, 23].

A question of considerable interest is the crossover point N at which large FCC crystalline structures become lower in energy that MIC structures. MIC structures have more favorable surface energies than FCC structures, but less favorable interior energies due to internal strains [12]. For sufficiently large N, the FCC bulk interior advantage overtakes the surface disadvantage. Van de Waal [23] relaxed an

increasing sequence of FCC tetrakaidecahedra using the full LJ potential to obtain an estimated MIC/FCC energy crossover point at $N = 3600$. Xie *et al.* [25] relaxed an increasing sequence of cuboctahedra (truncated octahedra with a cutting depth $f = \frac{1}{2}$) to obtain a crossover for that shape at N=10,179, and explicitly showed that the relaxed FCC cuboctahedron at N=10,179 is lower in energy than the relaxed closed shell Mackay icosahedron of the same size. Honeycutt and Andersen [11] relaxed approximately spherical FCC clusters to obtain an estimated crossover near $N = 5000$. However, these crossover values are larger than the experimental range of 1500 to 3500 suggested by electron diffraction studies of Argon clusters [16].

By considering the full LJ potential in the surface free energy calculation, the author has shown that the optimal truncated octahedral shape corresponds very closely to the value $f = \frac{2}{5}$, intermediate between the tetrakaidecahedron and the cuboctahedron [14]. This leads to a crossover value of approximately $N = 3000$, which can further be decreased to approximately $N = 2100$ by including (110) faces in the optimal shape. Using this shape, we have explicitly constructed an FCC cluster at $N = 2142$ (Figure 6) which is lower in energy than the best MIC cluster of the same size. We have also obtained essentially the same shape by applying the reverse greedy operator **R** over 2000 times in succession to a spherical FCC cluster near $N = 5000$. The optimal polyhedral Wulff shape quickly emerges from the spherical cluster as least tightly bound atoms are successively stripped away.

We have searched without success for other possible polyhedral FCC global optima in the microcluster range by considering all possible centrosymmetric truncated octahedra that correspond to rational values of f. The use of (110) planes, as well as relaxing the assumption of centrosymmetry, thus allowing planes with the same Miller indices to vary in distance from the origin, also has been considered. We now conjecture that there are no FCC global optima except **6** and **38** below $N = 2100$. Finally, we note the work of Raoult *et al.* [21], who relaxed various FCC polyhedra as well as multiply-twinned (unions of identical FCC polyhedra with shared faces) truncated decagonal FCC clusters. They conclude that the latter are lower in energy in the size range $N = 1600$ to 100,000, with pure FCC clusters of approximately the Wulff shape optimal for larger N. However, we note that the multiply twinned and pure FCC forms are very close in energy in this range, and the optimal sets for each may be interspersed over the intermediate region.

3. General Purpose Algorithms

There have been a wide variety of general purpose global optimization algorithms applied to GOLJC and other molecular conformation problems that do not make any prior assumptions regarding an underlying lattice structure. These algorithms incorporate various ideas and techniques, including simulated annealing, genetic algorithms, smoothing and spatial averaging of the objective function, and packet annealing, among others. We refer the reader to the excellent overview given in [20]

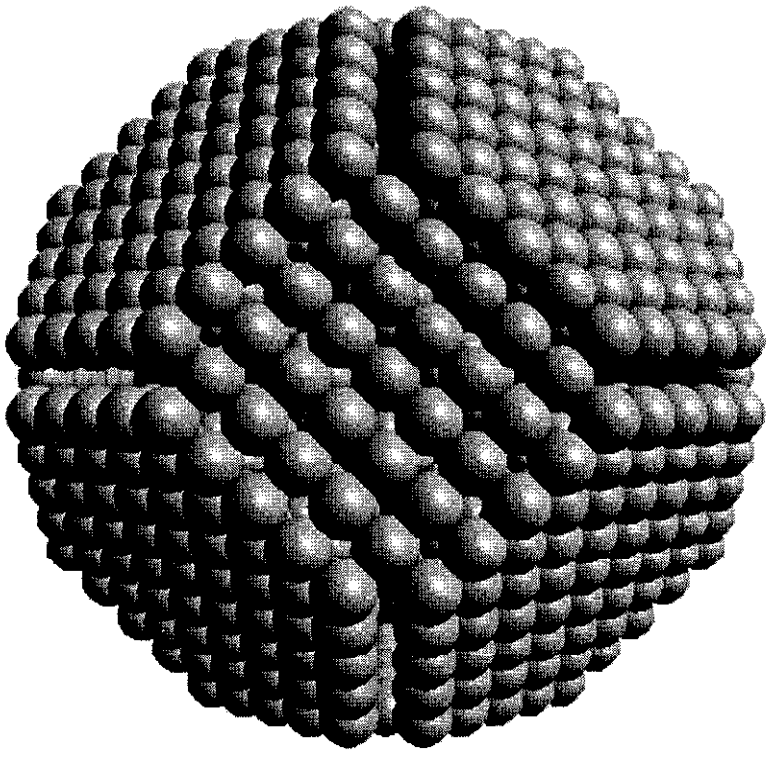

Figure 6. FCC configuration at $N = 2142$, lower in energy than the best MIC conformation of the same size.

for more details. Here we will briefly consider several algorithms that have proved successful in obtaining many of the results in Tables 1 and 2 over a significant range of N.

The algorithms of Coleman *et al.* [4] and Sloane *et al.* [22] both rely heavily on the generalized growth sequence operator. Starting with a pool of low lying local minima at $N-1$, candidate structures of size N are generated by **F**. Additional perturbational techniques are then employed on the resulting pool of clusters to attempt further improvement. The two algorithms have proved generally successful in obtaining most (but neither obtains all) of the MIC optimal structures in Tables 1 and 2 in the size ranges tested, as well as the HOC conformations **72** ([4] and [22]), and **75** [22]. However, neither algorithm finds any of the MISV structures, which can not be obtained by **F** since typically the pool of candidate conformations at $N-1$ have complete inner shells. They also fail to find the **38** FCC case, as the best $N = 37$ MIC structures are lower in energy than any adjacent $N = 37$ FCC

structure, and thus an $N = 37$ FCC structure is unlikely to ever be generated in the growth sequence.

The algorithm of Byrd *et al.* [3] is somewhat different in that it involves a global optimization over the coordinates of a single atom, but without using a growth sequence. Here an initial pool of candidate structures at size N is built from random configurations. In the first phase of the algorithm, each such configuration is successively improved by performing a 3-dimensional global optimization over the coordinates of the least tightly bound atom, with the best structure found then being relaxed. This is equivalent to first applying a reverse greedy step **R** without relaxing the resulting conformation of $N - 1$ atoms, immediately followed by a forward greedy step **F**. In the second phase of the algorithm, further improvements are attempted by first expanding the best candidate structures found in Phase I around their centers of mass by factors of up to 1.75. Both the least and second least tightly bound atoms are then selected for a more extensive (than in Phase I) single atom global optimization with respect to the expanded cluster. The best final candidates are relaxed to local optima. The method is successful in finding all the MIC lattice structures in Tables 1 and 2 for $N \leq 76$, as well as the **72** and **75** HOC conformations. However, as with the previous two build-up algorithms, the MISV conformation **69** and the FCC conformation **38** in the size range tested are not found.

More robust general purpose algorithms are required to find the FCC and MISV cases. One such algorithm is the genetic algorithm (GA) of Deaven *et al.* [6]. It has found almost all the global optima in Tables 1 and 2 for $N \leq 100$, including the FCC **38** conformation, four of the seven MISV conformations, and one of the two HOC conformations. The algorithm maintains a small (on the order of four or more) active population of relaxed structures. Unlike many GAs, the "crossover" operator is based on a geometric construction rather than a manipulation of bit strings. For each pair in the active population, a candidate child structure is generated by approximately halving each of the parent conformations with random planes through the centers of mass, and then assembling the child by glueing together one half from each parent. The child structure is then relaxed using a conjugate gradient algorithm. If the resulting structure is lower in energy than any member of the active population, it replaces that member. Since the child structure may be radically different from either parent, the algorithm avoids entering subclasses of structures from which it cannot readily escape or the global optimum is inaccessible.

We conclude with an overview of our own general purpose algorithm [15] which has produced all of the global optima up to $N = 70$, including the FCC and MISV cases. It is based on a simple random restart procedure in which a sequence of independent, random initial configurations are locally optimized by a two step algorithm. The putative global optimum is selected as the best local optimum

achieved during these trials.

The algorithm can be simply stated as follows:

Big Bang Algorithm:

Step 1. An initial configuration $x(0)$ in $3N$-dimensional space is randomly generated which each coordinate drawn independently from a normal distribution with mean 0 and standard deviation σ , where typically $\sigma \prec 0.05$. Thus the probability density of the starting points is spherically symmetric about the origin, and the points are tightly clustered there. Due to the close initial confinement, very high energies are observed (often on the order of 10^{18} or higher) for the starting configuration.

Step 2. An initial descent is performed using a sequence of fixed length steepest descent steps:

$$x(n+1) - x(n) - \lambda \nabla U(x(n))/ \parallel \nabla U(x(n)) \parallel \tag{9}$$

where $\parallel \cdot \parallel$ denotes the Euclidean norm and the step length $\lambda > 0$ is a parameter of the method. Note that

$$\parallel x(n+1) - x(n) \parallel = \lambda \tag{10}$$

so in general step 2 will not converge to a stationary point. The sequence of steepest descent steps is continued until is no further progress is made, as determined by the stopping criterion $U(x(n'+k)) > U(x(n'))$ for some some pre-chosen value of k (typically $k = 20$).

Step 3. The conformation $x(n')$ is relaxed by a conjugate gradient algorithm.

The typical behavior observed in Step 2 is for most of the atoms to flee radially outwards from the origin (the "big bang"), accompanied by rapid reduction in the potential function. As the expansion decelerates, more of the motion takes on a non-radial character. Step 2 terminates in the catchment region of a (hopefully) low-lying local minimum, which is then found in step 3.

A key parameter of the algorithm is the step length λ in step 2. We have found that $\lambda = 0.03$ works well in the microcluster range. Ideally it should be chosen small enough that the initial iterates are descent steps that eventually lead to the neighborhood of a low-lying local minimum, but large enough that the algorithm does not become trapped in higher-lying local minima. The hope is that when an iterate falls within the catchment region of such a higher minimum, the fixed length step will be long enough to escape to an improved potential function value in a lower-lying catchment region. Tests on the step 2 descent trajectory have indeed

shown that such catchment region hopping is occurring. Step 2 might be expected to be particularly successful if the energy landscape is analogous to a funnel with sides roughened by local optima with small catchment regions, but overall leading down to a few low-lying minima. We note that this funnel analogy has recently gained support as a characterization of the energy landscape of several protein folding problems [24].

The performance of the algorithm is shown in Figure 7, which shows a frequency graph of the number of times that the global optimum is hit for 100,000 independent random starting configurations as a function of N, with $\lambda = 0.03$ and $\sigma = 0.01$. Clearly the graph peaks near the closed-shell MIC magic numbers $N = 13$ and $N = 55$. Below $N = 55$, the algorithm is remarkably efficient. For example, at $N = 13$, it achieves a 85 percent hit rate on the global optimum, even though the number of local optima (and hence possible termination states) is known to be over 1000 [15]. At $N = 25$, the hit rate is still over 15 percent, even though the number of local optima is estimated at approximately 10^{10} by the Hoare formula [9]. The algorithm hits **38** at approximately a 1 in 330 rate, which is comparable to the results of Deaven *et al.* [6] who report that **38** is found after between 170 to 1000 mating operations with their genetic algorithm. However, above $N = 60$, the frequency falls to an impractically low value, and higher optima up to **70** have only been found by increasing the number of trials well above 100,000. When augmented with a perturbation step, in which less tightly bound atoms are recycled into the center of the cluster and Steps 2 and 3 repeated, the algorithm has found most of the global optima out to $N = 147$.

4. Concluding Remarks

Based on the results presented here, the geometric character of the global optima of Lennard-Jones clusters for both very small and very large N is believed to be well known. Somewhat less certain is the behavior in the intermediate region between MIC microclusters and FCC macroclusters. This intermediate range is well beyond the capabilities of current general purpose global optimizaton algorithms. Lattice-based algorithms are capable of generating results in this range, but there can be little confidence that their underlying bias toward structures of a given type will actually produce global optima.

The fact that fast, scalable algorithms based on lattice search and generalized growth sequence ideas are successful in locating most global optima in the microcluster range is highly encouraging and may bode well for future applications to protein folding problems. However, the example of the optimal FCC polyhedral cluster **38**, which apparently is out of reach of otherwise successful algorithms of this type, is a clear object lesson on the tradeoffs between generality and performance.

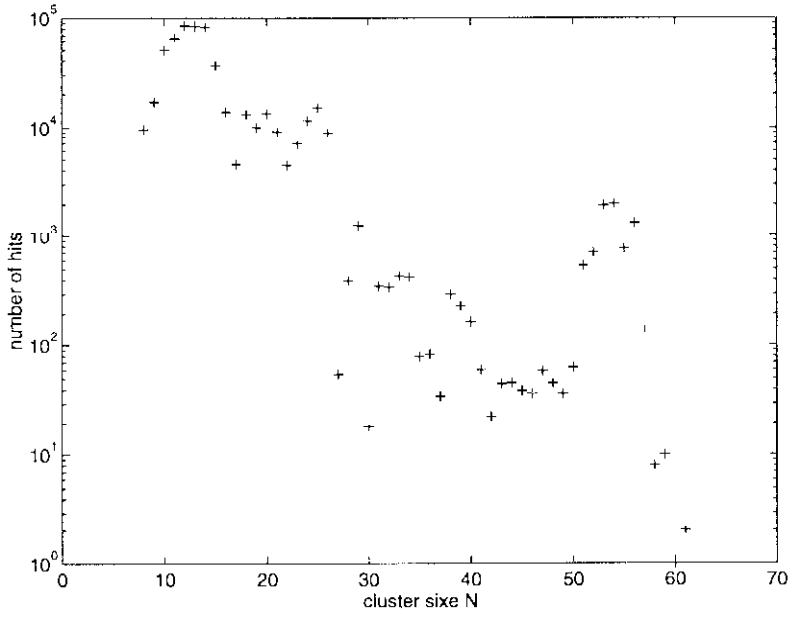

Figure 7. Number of global optima hits in 10^5 trials for the Big Bang algorithm

References

[1] C. Barron, S. Gomez, and D. Romero, Archimedean polyhedron structure yields a lower energy atomic cluster, *Applied Mathematics Letters*, Vol. 9-5(1996), pp. 75–78.

[2] G. C. Benson and T. A. Claxton, Estimation of surface energy of inert gas crystals, *Journal of the Physics and Chemistry of Solids*, Vol. 25(1964), pp. 367-378.

[3] R. H. Byrd, E. Eskow, and R. B. Schnabel, A new large-scale global optimization method and its application to Lennard-Jones problems, *Technical Report CU-CS-630-92*, Dept. of Computer Science, University of Colorado, revised 1995; also in P. M. Pardalos, D. Shalloway, G. Xue, editors, DIMACS Series in Discrete Mathematics and Theoretical Computer Science, Vol. 23, American Mathematical Society, Providence, R. I., 1996.

[4] T. F. Coleman, D. Shalloway, and Z. Wu, A parallel build-up algorithm for global energy minimizations of molecular clusters using effective energy simulated annealing, *Journal of Global Optimization*, Vol. 4(1994), pp. 171-185.

[5] H. M. S. Coxeter, Regular Polytopes (3d Ed.), Dover Publications, New York, 1973.

[6] D. M. Deaven, N. Tit, J. R. Morris, and K. M. Ho, Structural optimization of Lennard-Jones clusters by a genetic algorithm, *Chemical Physics Letters*, Vol. 256(1996), pp. 195–198.

[7] J. Farges, M. F. de Feraudy, B. Raoult, and G. Torchet, Non crystalline structure of argon clusters. II. Multilayer icosahedral structure of $Ar(N)$ clusters $50 < N < 750$, *Journal of Chemical Physics*, Vol. 84(1986), pp. 3491–3501.

[8] C. Herring, Some theorems on the free energies of crystal surfaces, *Physical Review*, Vol. 82(1951), pp. 87-93.

[9] M. R. Hoare, Structure and dynamics of simple microclusters, *Advances in Chemical Physics*, Vol. 40(1979), pp. 49–135.

[10] M. R. Hoare and P. Pal, Physical cluster mechanics: statics and energy surfaces for monatomic systems, *Advances in Physics*, Vol. 20(1971), pp. 161–196.

[11] J. D. Honeycutt and H. C. Andersen, Molecular dynamics study of melting and freezing of small Lennard-Jones clusters, *Journal of Physical Chemistry*, Vol. 91(1987), pp. 4950–4963.

[12] S. Ino, Stability of multiply-twinned particles, *Journal of the Physical Society of Japan*, Vol. 27(1969), pp. 941–953.

[13] C. Kittel, Introduction to Solid State Physics (7th Ed.), Wiley, New York, 1996.

[14] R. H. Leary, Optimal FCC polyhedral forms for large-scale Lennard-Jones clusters, manuscript in preparation.

[15] R. H. Leary, A robust gradient descent algorithm for the global optimization of Lennard-Jones clusters, *Technical Report GA-A-22514*, San Diego Supercomputer Center, San Diego, 1996.

[16] J. W. Lee and G. D. Stein, Electron diffraction experiments on argon clusters nucleated in helium using laval nozzle beams, *Surface Science*, Vol. 156(1985), pp. 112-120.

[17] A. L. Mackay, A dense non-crystallographic packing of equal spheres, *Acta Crystallographica*, Vol. 15(1962), pp. 916-918.

[18] W. Miehle, O. Kandler, T. Leisner, and O. Echt, Mass spectrometric evidence for icosahedral structure in large rare gas clusters: Ar, Kr, Xe, *Journal of Chemical Physics*, Vol. 91(1989), pp. 5940-5952.

[19] J. A. Northby, Structure and binding of Lennard-Jones clusters: $13 \leq N \leq 147$, *Journal of Chemical Physics*, Vol. 87(1987), pp. 6166-6178.

[20] P.M. Pardalos, D. Shalloway and G.L. Xue, Optimization methods for computing global minima of non-convex potential energy functions, *Journal of Global Optimization*, Vol. 4(1994), pp. 117-133.

[21] B. Raoult, J. Farges, M. F. De Feraudy, and G. Torchet, Comparison between icosahedral, decahedral, and crystalline Lennard-Jones models containing 500 to 6000 atoms, *Philosophical Magazine B*, Vol. 60(1989), pp. 881 906.

[22] N. J. A. Sloane, R. H. Hardin, T. D. S. Duff, and J. H. Conway, Minimal energy clusters of hard spheres, *Discrete and Computational Geometry*, Vol. 14(1995), pp. 237–259.

[23] D. W. van de Waal, Stability of face-centered cubic and icosahedral Lennard Jones clusters, *Journal of Chemical Physics*, Vol. 90(1989), pp. 3407–3408.

[24] P. Wolynes, J. Onuchic, and D.Thirumalai, Navigating the folding routes, *Science*, Vol. 267(1995), pp. 1619-1620.

[25] J. Xie, J. A. Northby, D. L. Freeman, and J. D. Doll, Theoretical studies of the energetics and structure of atomic clusters, *Journal of Chemical Physics*, Vol. 91(1989), pp. 612-619.

[26] G.L. Xue, Molecular conformation on the CM-5 by parallel two-level simulated annealing, *Journal of Global Optimization*, Vol. 4(1994), pp. 187–208.

[27] G.L. Xue, Improvement of the Northby algorithm for molecular conformation: better solutions, *Journal of Global Optimization*, Vol. 4(1994), pp. 425–440.